
Vertical Distribution and Kinematics of Protoplanetary Nebulae in the Galaxy

V.V. Bobylev¹ and A.T. Bajkova

*Central (Pulkovo) Astronomical Observatory, Russian Academy of Sciences,
Pulkovskoe sh. 65, St. Petersburg, 196140 Russia*

Abstract—The catalogue of protoplanetary nebulae by Vickers et al. has been supplemented with the line-of-sight velocities and proper motions of their central stars from the literature. Based on an exponential density distribution, we have estimated the vertical scale height from objects with an age less than 3 Gyr belonging to the Galactic thin disk (luminosities higher than $5000 L_{\odot}$) to be $h = 146 \pm 15$ pc, while from a sample of older objects (luminosities lower than $5000 L_{\odot}$) it is $h = 568 \pm 42$ pc. We have produced a list of 147 nebulae in which there are only the line-of-sight velocities for 55 nebulae, only the proper motions for 25 nebulae, and both line-of-sight velocities and proper motions for 67 nebulae. Based on this kinematic sample, we have estimated the Galactic rotation parameters and the residual velocity dispersions of protoplanetary nebulae as a function of their age. We have established that there is a good correlation between the kinematic properties of nebulae and their separation in luminosity proposed by Vickers. Most of the nebulae are shown to be involved in the Galactic rotation, with the circular rotation velocity at the solar distance being $V_0 = 227 \pm 23$ km s⁻¹. The following principal semiaxes of the residual velocity dispersion ellipsoid have been found: $(\sigma_1, \sigma_2, \sigma_3) = (47, 41, 29)$ km s⁻¹ from a sample of young protoplanetary nebulae (with luminosities higher than $5000 L_{\odot}$), $(\sigma_1, \sigma_2, \sigma_3) = (50, 38, 28)$ km s⁻¹ from a sample of older protoplanetary nebulae (with luminosities of $4000 L_{\odot}$ or $3500 L_{\odot}$), and $(\sigma_1, \sigma_2, \sigma_3) = (91, 49, 36)$ km s⁻¹ from a sample of halo nebulae (with luminosities of $1700 L_{\odot}$).

DOI: 10.1134/S1063773717070027

INTRODUCTION

At present, the stars surrounded by gas–dust shells in a brief transition phase from asymptotic giant branch (AGB) stars to planetary nebulae are being actively studied. These are stars that have already ceased to lose their mass on the AGB but have not yet become hot enough to ionize the remnants of the shells surrounding them. The universally accepted name of this evolutionary phase is protoplanetary nebulae (PPNe) or post-asymptotic giant branch (post-AGB) stars. However, the mass loss continues even after the end of thermal pulsations in the post-AGB star. In particular, white dwarfs, the central stars of planetary nebulae, lose their mass with a rate of $\sim 10^{-10} M_{\odot} \text{ yr}^{-1}$.

A large number of PPN candidates have been revealed (Garcia-Lario et al. 1997) by infrared observations from the Infra-Red Astronomical Satellite (IRAS) (Neugebauer et al.

¹e-mail: vbobylev@gao.spb.ru

1984). The membership in the PPN class for most of them has been confirmed relatively recently by analyzing their ground based optical spectra (Garcia-Lario 2006; Suárez et al. 2006). The most complete up-to-date information on PPNe in the Milky Way is contained in the Toruń catalogue (Szczerba et al. 2007, 2012).

The shell expansion is believed to be spherically symmetric at the AGB phase (Habing and Olofsson 2003). However, at the post-AGB phase, apart from a more or less symmetric shell, collimated high velocity bipolar jets are observed in the radio band (Pérez-Sánchez et al. 2013). The environment in the shells and jets is favorable for the emergence of maser emission (Gómez et al. 2015). Highly accurate measurements of the trigonometric parallaxes have already been performed with ground-based very-long baseline interferometers for some post-AGB objects (Imai et al. 2007, 2013).

In particular, stars with OH/IR maser emission (some of which are post-AGB stars) play an important role in studying the structure and kinematics of the Galaxy. For example, Debattista et al. (2002) estimated the rotation velocity of the central bar using radio observations of 250 OH/IR stars. In Gesicki et al. (2014) post-AGB stars served to study the star formation history in the Milky Way bulge.

Based on three density distributions and using data on planetary nebulae from the catalogues by Frew (2008) and Stanghellini and Haywood (2010), Bobylev and Bajkova (2017) found the vertical disk scale height and determined the Galactic rotation parameters. Obviously, estimating these parameters from a sample of objects at an earlier evolutionary phase is of interest. At present, it has become possible to perform such a study owing to the catalogue by Vickers et al. (2015), which contains 209 PPNe and 87 candidates. Quite reliable distance estimates have been obtained for all these objects by fitting the observed spectral energy distribution to the blackbody one. For so an extensive sample of PPNe such a homogeneous distance scale has been realized by Vickers et al. (2015) for the first time.

The goal of this paper is to study the z distribution and kinematics of PPNe in the Galaxy based on the catalogue by Vickers et al. (2015). This suggests solving the following problems: estimating the scale height, producing a sample with measured line-of-sight velocities and proper motions, and estimating the Galactic rotation parameters and the residual velocity dispersions for PPNe as a function of their age or membership in such Galactic subsystems as the thin disk, the thick disk, or the halo.

METHODS

In this paper we use a rectangular Galactic coordinate system with the axes directed away from the Sun toward the Galactic center ($l = 0^\circ, b = 0^\circ$, the x axis or axis 1), in the direction of Galactic rotation ($l = 90^\circ, b = 0^\circ$, the y axis or axis 2), and toward the north Galactic pole ($b = 90^\circ$, the z axis or axis 3).

We know three stellar velocity components from observations: the line-of-sight velocity V_r and the two tangential velocity components $V_l = 4.74r\mu_l \cos b$ and $V_b = 4.74r\mu_b$ along the Galactic longitude l and latitude b , respectively, expressed in km s^{-1} . Here, the coefficient 4.74 is the ratio of the number of kilometers in an astronomical unit to the number of seconds in a tropical year, and r is the stellar heliocentric distance in kpc. The proper motion components $\mu_l \cos b$ and μ_b are expressed in mas yr^{-1} . The velocities U, V, W directed along the x, y, z

coordinate axes are calculated via the components V_r, V_l, V_b , respectively:

$$\begin{aligned} U &= V_r \cos l \cos b - V_l \sin l - V_b \cos l \sin b, \\ V &= V_r \sin l \cos b + V_l \cos l - V_b \sin l \sin b, \\ W &= V_r \sin b + V_b \cos b. \end{aligned} \quad (1)$$

Note that when the residual velocity dispersions are calculated, the velocities U, V, W must be freed from the group motion of the stars relative to the Sun ($U_\odot, V_\odot, W_\odot$) and from the differential Galactic rotation effects.

The Velocity Dispersion Ellipsoid

In this paper we use the following well-known method (Trumpler and Weaver 1953; Ogorodnikov 1965) to estimate the residual velocity dispersions for the PPN sample. We consider six second-order moments a, b, c, f, e , and d :

$$\begin{aligned} a &= \langle U^2 \rangle - \langle U_\odot^2 \rangle, \\ b &= \langle V^2 \rangle - \langle V_\odot^2 \rangle, \\ c &= \langle W^2 \rangle - \langle W_\odot^2 \rangle, \\ f &= \langle VW \rangle - \langle V_\odot W_\odot \rangle, \\ e &= \langle WU \rangle - \langle W_\odot U_\odot \rangle, \\ d &= \langle UV \rangle - \langle U_\odot V_\odot \rangle, \end{aligned} \quad (2)$$

which are the coefficients of the surface equation

$$ax^2 + by^2 + cz^2 + 2fyz + 2ezx + 2dxy = 1, \quad (3)$$

and the components of the symmetric residual velocity moment tensor

$$\begin{pmatrix} a & d & e \\ d & b & f \\ e & f & c \end{pmatrix}. \quad (4)$$

The following six equations are used to determine the values of this tensor from observations:

$$\begin{aligned} V_r^2 &= a \cos^2 b \cos^2 l + b \cos^2 b \sin^2 l + c \sin^2 b \\ &+ 2f \cos b \sin b \sin l + 2e \cos b \sin b \cos l + 2d \sin l \cos l \cos^2 b, \end{aligned} \quad (5)$$

$$V_l^2 = a \sin^2 l + b \cos^2 l \sin^2 l - 2d \sin l \cos l, \quad (6)$$

$$\begin{aligned} V_b^2 &= a \sin^2 b \cos^2 l + b \sin^2 b \sin^2 l + c \cos^2 b \\ &- 2f \cos b \sin b \sin l - 2e \cos b \sin b \cos l + 2d \sin l \cos l \sin^2 b, \end{aligned} \quad (7)$$

$$\begin{aligned} V_l V_b &= a \sin l \cos l \sin b + b \sin l \cos l \sin b \\ &+ f \cos l \cos b - e \sin l \cos b + d(\sin^2 l \sin b - \cos^2 l \sin b), \end{aligned} \quad (8)$$

$$\begin{aligned} V_b V_r &= -a \cos^2 l \cos b \sin b - b \sin^2 l \sin b \cos b + c \sin b \cos b \\ &+ f(\cos^2 b \sin l - \sin l \sin^2 b) + e(\cos^2 b \cos l - \cos l \sin^2 b) \\ &- d(\cos l \sin l \sin b \cos b + \sin l \cos l \cos b \sin b), \end{aligned} \quad (9)$$

$$\begin{aligned} V_l V_r &= -a \cos b \cos l \sin l + b \cos b \cos l \sin l \\ &+ f \sin b \cos l - e \sin b \sin l + d(\cos b \cos^2 l - \cos b \sin^2 l), \end{aligned} \quad (10)$$

which are solved by the least-squares method for the six unknowns a, b, c, f, e , and d . The eigenvalues of the tensor (4) $\sigma_{1,2,3}$ are then found from the solution of the secular equation

$$\begin{vmatrix} a - \lambda & d & e \\ d & b - \lambda & f \\ e & f & c - \lambda \end{vmatrix} = 0. \quad (11)$$

The eigenvalues of this equation are known to be equal to the reciprocals of the squares of the semiaxes of the velocity moment ellipsoid and, at the same time, the squares of the semiaxes of the residual velocity ellipsoid:

$$\begin{aligned} \lambda_1 &= \sigma_1^2, \lambda_2 = \sigma_2^2, \lambda_3 = \sigma_3^2, \\ \lambda_1 &> \lambda_2 > \lambda_3. \end{aligned} \quad (12)$$

The directions of the principal axes of the tensor (11), $L_{1,2,3}$ and $B_{1,2,3}$ are found from the relations

$$\text{tg } L_{1,2,3} = \frac{ef - (c - \lambda)d}{(b - \lambda)(c - \lambda) - f^2}, \quad (13)$$

$$\text{tg } B_{1,2,3} = \frac{(b - \lambda)e - df}{f^2 - (b - \lambda)(c - \lambda)} \cos L_{1,2,3}. \quad (14)$$

The Galactic Rotation Curve

To determine the parameters of the Galactic rotation curve, we use the equations derived from Bottlinger's formulas in which the angular velocity Ω is expanded into a series to terms of the second order of smallness in r/R_0 :

$$\begin{aligned} V_r &= -U_\odot \cos b \cos l - V_\odot \cos b \sin l - W_\odot \sin b \\ &+ R_0(R - R_0) \sin l \cos b \Omega'_0 + 0.5R_0(R - R_0)^2 \sin l \cos b \Omega''_0, \end{aligned} \quad (15)$$

$$\begin{aligned} V_l &= U_\odot \sin l - V_\odot \cos l - r\Omega_0 \cos b \\ &+ (R - R_0)(R_0 \cos l - r \cos b) \Omega'_0 + 0.5(R - R_0)^2(R_0 \cos l - r \cos b) \Omega''_0, \end{aligned} \quad (16)$$

$$\begin{aligned} V_b &= U_\odot \cos l \sin b + V_\odot \sin l \sin b - W_\odot \cos b \\ &- R_0(R - R_0) \sin l \sin b \Omega'_0 - 0.5R_0(R - R_0)^2 \sin l \sin b \Omega''_0, \end{aligned} \quad (17)$$

where Ω_0 is the angular velocity of Galactic rotation at the Galactocentric distance R_0 of the Sun, the parameters Ω'_0 and Ω''_0 are the first and second derivative of the angular velocity, respectively, $V_0 = |R_0\Omega_0|$, and R is the distance from the star to the Galactic rotation axis calculated from the formula

$$R^2 = r^2 \cos^2 b - 2R_0r \cos b \cos l + R_0^2. \quad (18)$$

We need to know the specific value of the distance R_0 . Gillessen et al. (2009) obtained one of its most reliable estimates, $R_0 = 8.28 \pm 0.29$ kpc, by analyzing the orbits of stars moving around the massive black hole at the Galactic center. The following estimates were obtained from various samples of masers with measured trigonometric parallaxes: $R_0 = 8.34 \pm 0.16$ (Reid et al. 2014), 8.3 ± 0.2 (Bobylev and Bajkova 2014), 8.03 ± 0.12 (Bajkova and Bobylev 2015), and 8.24 ± 0.12 kpc (Rastorguev et al. 2017). Based on these estimates, we adopted $R_0 = 8.3 \pm 0.2$ kpc in this paper.

DATA

The Catalogue by Vickers et al. (2015)

Basic information about 326 probable PPNe in the Milky Way and 107 candidates is collected in the Toruń catalogue (Szczerba et al. 2007, 2012), which is most complete to date. It contains data on the classification, coordinates, and photometry of each object.

In this paper we use the distance estimates from the catalogue by Vickers et al. (2015). It contains 209 PPNe and 87 candidates from the Toruń catalogue. The distances to the objects were determined by fitting the observed spectral energy distribution to the blackbody one. The infrared photometric and spectroscopic data from many sources (more than 20 catalogues) obtained in both ground-based (for example, DENIS, 2MASS, UKIDSS) and spaceborne (for example, IRAS, IUE, ISO, Planck, WISE) observations were used for this purpose.

The Kinematic Sample

When producing the kinematic sample to study the spatial distribution and kinematics of PPNe in the Galaxy, we ran into the problem that information about the line-of-sight velocities of their central stars was presented quite poorly in the SIMBAD¹ electronic database. At the same time, there are many publications where for individual objects information about their systemic line-of-sight velocities is available. These include, for example, the papers by Klochkova et al. (1999, 2007, 2014, 2015), Klochkova (2013), Arkhipova et al. (2001), or Sánchez Contreras and Sahai (2012). The bibliographic reviews with the line-of-sight velocities of PPNe (Yoon et al. 2014) and OH masers (Deacon et al. 2004; Engels and Bunzel 2016) turned out to be useful.

We took the proper motions from such catalogues as Hipparcos (1997) revised by van Leeuwen (2007), TRC (Hog et al. 1998), Tycho-2 (Hog et al. 2000), and the UCAC catalogues (Zacharias et al. 2004, 2010, 2013).

Our list contains a total of 147 nebulae (we combined the lists of PPNe and the lists of candidates from the catalogue by Vickers et al. (2015)). It contains either only the line-of-sight velocities (55 nebulae), or only the proper motions (25 nebulae), or both line-of-sight velocities and proper motions (67 nebulae). The first ten PPNe from our list are given in Table 1 (the remaining ones are accessible in the electronic publication of the catalogue):

- Column 1 gives the IRAS number;
- 2—an alternative designation of the object;
- 3 and 4—the Galactic coordinates l and b copied from the catalogue by Vickers et al. (2015);
- 5—the PPN luminosity Lum (in solar luminosities) copied from the catalogue by Vickers et al. (2015);
- 6—the heliocentric distance r and its error σ_r copied from the catalogue by Vickers et al. (2015);
- 7 and 8—the equatorial coordinates α ($J2000.0$) and δ ($J2000.0$), taken from the SIMBAD electronic database;
- 9 and 10—the proper motion components $\mu_\alpha \cos \delta$ and μ_δ taken from various sources;
- 11 and 12—the random measurement errors of the proper motion components $\sigma_{\mu_\alpha \cos \delta}$ and σ_{μ_δ} ;

¹<http://simbad.u-strasbg.fr/simbad>

Таблица 1: Data on the PPNe

IRAS	Another designation	l deg	b deg	Lum	$r \pm \sigma_r$ kpc	$\alpha(J2000.0)$ h, m, s	$\delta(J2000.0)$ °, m, s		
1	2	3	4	5	6	7	8		
	LS 4825	1.671	-6.628	4000	6.45 ± 1.36	18 16 00.470	-30 45 23.25		
18371-3159	LSE 63	2.918	-11.818	1700	5.34 ± 1.30	18 40 22.017	-31 56 48.82		
17074-1845	LSE 3	4.100	12.263	6000	6.88 ± 1.18	17 10 24.148	-18 49 00.67		
18384-2800	V4728 Sgr	6.725	-10.372	4000	2.29 ± 0.62	18 41 36.961	-27 57 01.25		
F16277-0724	LS IV-07 1	7.956	26.706	3500	0.91 ± 0.20	16 30 30.018	-07 30 52.03		
17203-1534	LS IV-15 3	8.548	11.486	6000	6.42 ± 0.95	17 23 11.916	-15 37 15.06		
17279-1119	V340 Ser	13.230	12.174	6000	3.43 ± 0.47	17 30 46.925	-11 22 08.28		
	LS IV-04 1	14.403	22.856	1700	6.86 ± 1.53	16 56 27.730	-04 47 23.70		
F15240+1452	BD+15 2862	21.866	51.930	1700	1.43 ± 0.33	15 26 20.818	+14 41 36.32		
19500-1709	V5112 Sgr	23.984	-21.036	6000	2.42 ± 0.31	19 52 52.701	-17 01 50.30		
$\mu_\alpha \cos \delta$ mas yr ⁻¹	μ_δ mas yr ⁻¹	$\sigma_{\mu_\alpha \cos \delta}$ mas yr ⁻¹	σ_{μ_δ} mas yr ⁻¹	Source of μ	V_r km s ⁻¹	σ_{V_r} km s ⁻¹	Source of V_r	Spectral type	...
9	10	11	12	13	14	15	16	17	18–20
-2.7	-6.9	3.0	3.0	Tyc2	-0.8		(1)	B1Ib	...
-5.2	-6.0	3.5	3.0	Tyc2	10.7	1.0	(2)	B1Iabe	...
-4.8	-9.2	2.8	2.6	Tyc2	12.4	1.5	(2)	B5Ibe	...
3.0	-5.1	1.6	1.5	Tyc2	-85.0	5.0	(3)	F2/3Ia+M?	...
3.6	1.6	0.4	0.3	Hip	2.3	2.0	(4)	A9II/III	...
-6.8	-7.2	2.2	2.2	Tyc2	51.4	2.1	(2)	B1IIIpe	...
-2.5	-3.8	1.5	1.4	Tyc2	68.7		(5)	F2/3II	...
1.5	-4.9	0.6	0.5	Chen	89.3		(6)	B	...
8.9	-10.9	0.5	0.6	Hip	-45.0	3.7	(7)	B9Iab:p	...
-2.7	-3.8	1.4	1.4	Tyc2	13.0		(8)	F2/3(Iab+A)p	...

The PPN luminosity Lum is given in solar luminosities, Chen–Chen et al. (2000), (1)–Ryans (1997), (2)–Mello et al. (2012), (3)–Reyniers and van Winckel (2001), (4)–Evans (1979), (5)–Rao et al. (2012), (6)–Mooney et al. (2002), (7)–Kharchenko et al. (2007), (8)–Klochkova (2013).

13—the designation of the catalogues of proper motions;

14 and 15—the heliocentric line-of-sight velocity V_r and its measurement error σ_{V_r} (if it is available), below, for example, when assigning the weights to the equations if there was no estimate of the line-of-sight velocity error, we assumed $\sigma_{V_r} = 5 \text{ km s}^{-1}$;

16—the reference to the line-of-sight velocity source;

17—the spectral type (if it is available) mainly from the SIMBAD electronic database.

18, 19, and 20—the parallax and proper motion components (all with the corresponding errors) from the Gaia DR1 catalogue (Prusti et al. 2016).

RESULTS AND DISCUSSION

The z Distribution

We analyzed the vertical distribution of PPNe using two samples. To produce them, we divided all 296 objects into two approximately equal parts by the luminosity specified in the catalogue by Vickers et al. (2015). Sample 1 includes nebulae with a luminosity higher than $5000 L_\odot$, while sample 2 includes older nebulae with a luminosity lower than $5000 L_\odot$. The luminosities in the catalogue by Vickers et al. (2015) have the following values: $20000 L_\odot$, $15000 L_\odot$, $12000 L_\odot$, $6000 L_\odot$, $4000 L_\odot$, $3500 L_\odot$ and $1700 L_\odot$. According to Table 2 from the paper of these authors, our sample 1 consists of Galactic thin-disk objects with an age less than 3 Gyr, i.e., of relatively young objects. Sample 2 has a more complex structure. It can include old thin-disk objects, thick-disk and bulge objects, and halo objects. In addition, we specified a constraint on the heliocentric distances, which must not exceed 6 kpc. With this condition we eliminate the objects subjected to the disk warp in sample 1 and the bulge objects in sample 2.

To describe the observed frequency distribution of objects along the z coordinate axis, we apply the model of an exponential density distribution:

$$N(z) = N_0 \exp\left(-\frac{|z - z_\odot|}{h}\right), \quad (19)$$

where N_0 is the normalization coefficient, z_\odot is the distance from the Sun to the Galactic midplane (the mean of the z coordinates of all objects from the sample), and h is the vertical disk scale height. The results of our analysis of samples 1 and 2 are reflected in the upper part of Table 2, where the derived parameters of the exponential distribution (19) are given, and in Fig. 1, where the histograms of the z distributions of PPNe are constructed. The results of our analysis of several objects characterizing the properties of the Galactic disk are presented in the lower part of Table 2.

As we can see from Table 2, z_\odot is determined from PPNe with very large errors. This parameter is determined much more accurately from other classes of young Galactic thin-disk objects, for example, hydrogen clouds, young open star clusters (OSCs), or OB stars. For example, Bobylev and Bajkova (2016) calculated $z_\odot = -16 \pm 2 \text{ pc}$ as a mean of the results obtained from a number of young objects (OB associations, Wolf–Rayet stars, HII regions, and Cepheids). Buckner and Froebrich (2014) found $z_\odot = -18.5 \pm 1.2 \text{ pc}$ from their analysis of OSCs.

Note that based on clusters of various ages and using an exponential density distribution, Buckner and Froebrich (2014) traced the behavior of the scale height h as a function of the cluster age and position in the Galaxy. The value of $h = 146 \pm 15 \text{ pc}$ we found is in agreement

Таблица 2: Parameters z_{\odot} and h

Objects	N_{\star}	z_{\odot} , pc	h , pc	Reference
PPNe, sample 1	107	-28 ± 12	146 ± 15	this paper
PPNe, sample 2	88	-37 ± 53	568 ± 42	this paper
OSCs	—	-18.5 ± 1.2	—	(1)
Various young objects	—	-16 ± 2	—	(2)
OSCs, 200–1000 Myr	—	-15 ± 2	150 ± 27	(3)
Planetary nebulae	230	-6 ± 7	197 ± 10	(4)
White dwarfs	717	—	220–300	(5)
Old thin-disk stars	1×10^4	-27 ± 4	330 ± 3	(6)
Oldest disk stars, APOGEE, $[\text{Fe}/\text{H}] \sim -0.5$ dex	1×10^3	—	~ 800	(7)

N_{\star} is the number of objects used, (1) Buckner and Froebrich (2014), (2) Bobylev and Bajkova (2016), (3) Bonatto et al. (2006), (4) Bobylev and Bajkova (2017), (5) Vennes et al. (2002), (6) Chen et al. (2001), (7) Bovy et al. (2016).

with $h = 150 \pm 27$ pc obtained by Bonatto et al. (2006) from open stars clusters with ages in the range 200–1000 Myr or with $h = 146 \pm 36$ pc found by Buckner and Froebrich (2014) from clusters of the MWSC (Milky Way Star Clusters) catalogue (Kharchenko et al. 2013) with a mean age of ~ 1 Gyr. Bobylev and Bajkova (2017) found $h = 197 \pm 10$ pc from a sample of planetary nebulae. Thus, a scale height $h \sim 150$ pc is typical for the mature population of the Galactic thin disk.

When the Galactic disk is arbitrarily divided into the thin and thick ones, scale heights $h \sim 150 - 250$ pc and ~ 700 pc are assumed to be typical for the thin and thick disks, respectively. The view that there is no distinct thick disk, no bimodality, but there is one evolving disk has been strengthened in recent years (Bovy et al. 2012; Rix and Bovy 2013; Bovy et al. 2016). Bovy et al. (2016) thoroughly studied a large sample of red clump giants with various chemical compositions from the APOGEE (Apache Point Observatory Galactic Evolution Experiment) survey (Majewski et al. 2016). The value of $h = 568 \pm 42$ pc that we found from sample 2 is intermediate between the extreme values, h from 150 to 900 pc (Bovy et al. 2016), and shows that this population has a mature age and is fairly heated kinematically.

Note that the histogram constructed from old PPNe appears asymmetric (Fig. 1b). This may be because the sample itself is inhomogeneous. The scale heights separately from the southern ($z < 0$ pc) and northern ($z > 0$ pc) parts of sample 2 are $h = 590 \pm 54$ pc at $z < 0$ pc and $h = 607 \pm 33$ pc at $z > 0$ pc.

Galactic Rotation

In the case where all components of the space velocities are known, the circular rotation velocity V_{circ} of a nebula around the Galactic rotation axis is found from the relation

$$V_{\text{circ}} = U \sin \theta + (V_0 + V) \cos \theta, \quad (20)$$

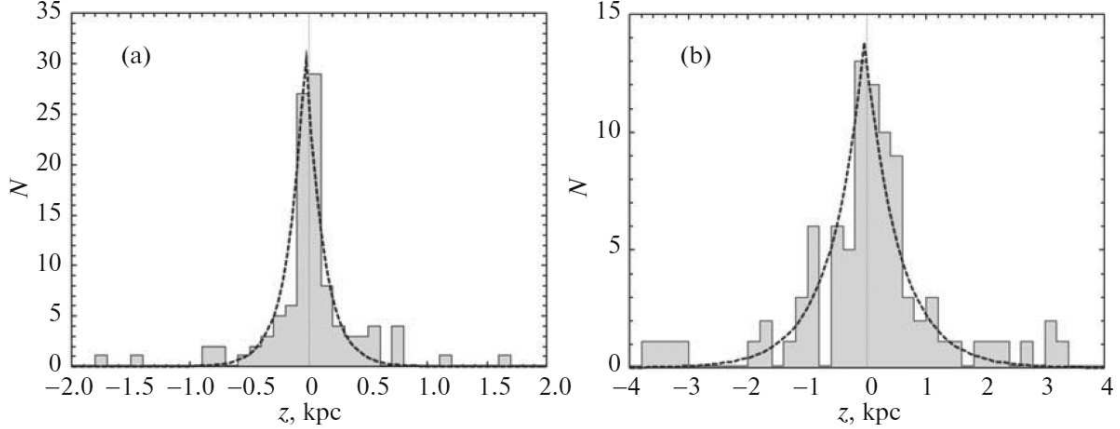


Рис. 1: Histogram of the z distribution of relatively younger PPNe (a) and older PPNe (b). The dashed line represents the model (19) constructed with the parameters from Table 2.

where $V_0 = |R_0\Omega_0|$ and the position angle θ obeys the relation $\text{tg } \theta = y/(R_0 - x)$. If, however, only the line-of-sight velocity is known for a nebula, then V_{circ} is calculated from the formula

$$V_{\text{circ}} = |R\Omega_0| + RV_r/(R_0 \sin l \cos b). \quad (21)$$

Figure 2 presents the circular rotation velocities V_{circ} of PPNe estimated from their total space velocities using Eq. (20) with the adopted V_0 and the rotation velocities of other nebulae constructed only from their line-of-sight velocities using Eq. (21). The Galactic rotation curve obtained by Reid et al. (2014) based on their analysis of ~ 100 Galactic masers with measured trigonometric parallaxes is also plotted here. This rotation curve is described by the relation $V_{\text{circ}} = V_0 - 0.2(R - R_0) \text{ km s}^{-1}$. It is clearly seen to be close to a flat one with a constant rotation velocity V_{circ} . Figure 2 shows the second, more complex Galactic rotation curve. The parameters of this curve were found by Bobylev and Bajkova (2013) by fitting the Allen–Santillán three-component model gravitational Galactic potential (Allen and Santillán 1991) to the data on masers with measured trigonometric parallaxes. In both Reid et al. (2014) and Bobylev and Bajkova 2013) the rotation velocity of the solar neighborhood V_0 is close to 240 km s^{-1} at $R_0 = 8.3 \text{ kpc}$. More accurate values of V_{circ} can be obtained if V_0 is estimated more accurately from the kinematics of PPNe themselves.

We considered three samples with different luminosity indices Lum . As can be seen from the figure, except for the bulge region ($R < 4 \text{ kpc}$), most of the PPNe are involved in the Galactic rotation. There are quite a few objects with rapid rotation ($V_{\text{circ}} \sim 220 \text{ km s}^{-1}$) even in the sample with luminosities of $1700 L_\odot$, which, according to Vickers et al. (2015), are halo objects.

To study the kinematic properties of nebulae, we produced a catalog of their residual velocities. It includes 67 PPNe for which all three components of the space velocity are known. We took the group velocity components $(U_\odot, V_\odot, W_\odot) = (11.5, 28.0, 3.7) \pm (3.4, 4.8, 6.7) \text{ km s}^{-1}$ found by Bobylev and Bajkova (2017) from their analysis of planetary nebulae and took the flat curve from Reid et al. (2014) as the Galactic rotation curve. The results are presented in Fig. 3, where the derived residual space velocities of PPNe on the UV , UW , and VW planes are shown. We can see from this figure that there are two populations of points. The first (most numerous) population is concentrated in a small central region

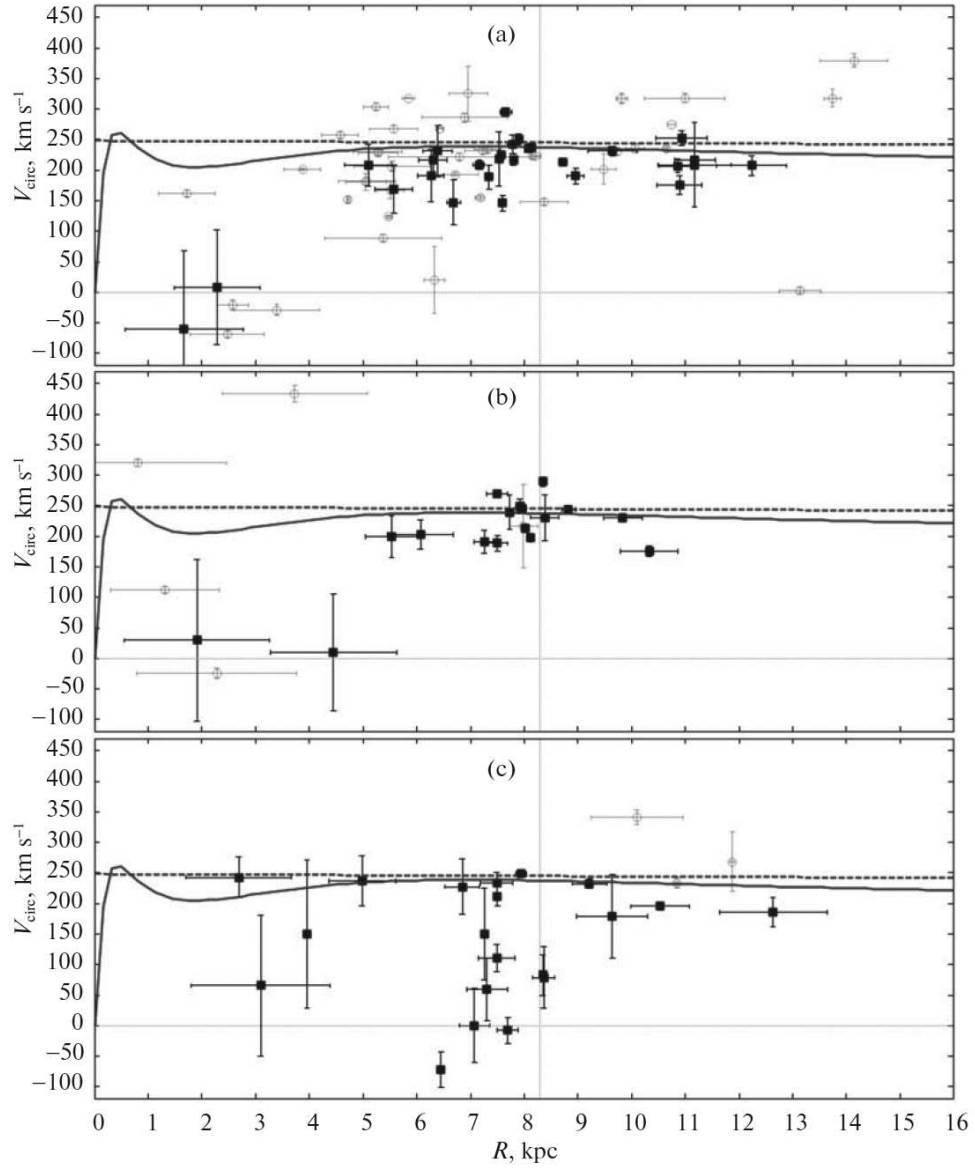


Рис. 2: Estimates of the circular rotation velocities V_{circ} for PPNe with luminosities higher than $5000 L_{\odot}$ (a), luminosities of $4000 L_{\odot}$ and $3500 L_{\odot}$ (b), and luminosities of $1700 L_{\odot}$ (c); those obtained from the total space velocities (filled squares), those constructed from the nebulae only with the line-of-sight velocities (open circles), the Galactic rotation curve from Reid et al. (2014) is indicated by the thick dashed line, the Galactic rotation curve from Bobylev and Bajkova (2013) is indicated by the thick solid line, the vertical dotted line marks the Sun's position.

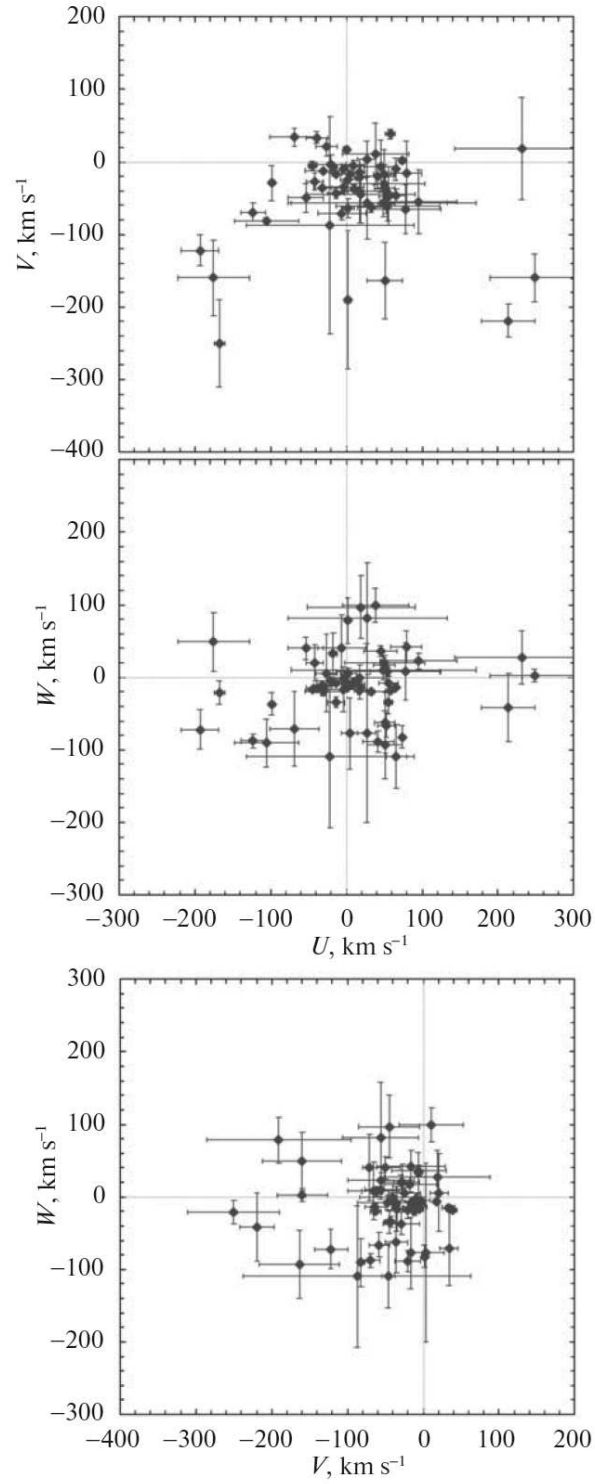


Рис. 3: Residual velocities of PPNe on the UV , UW , and VW planes.

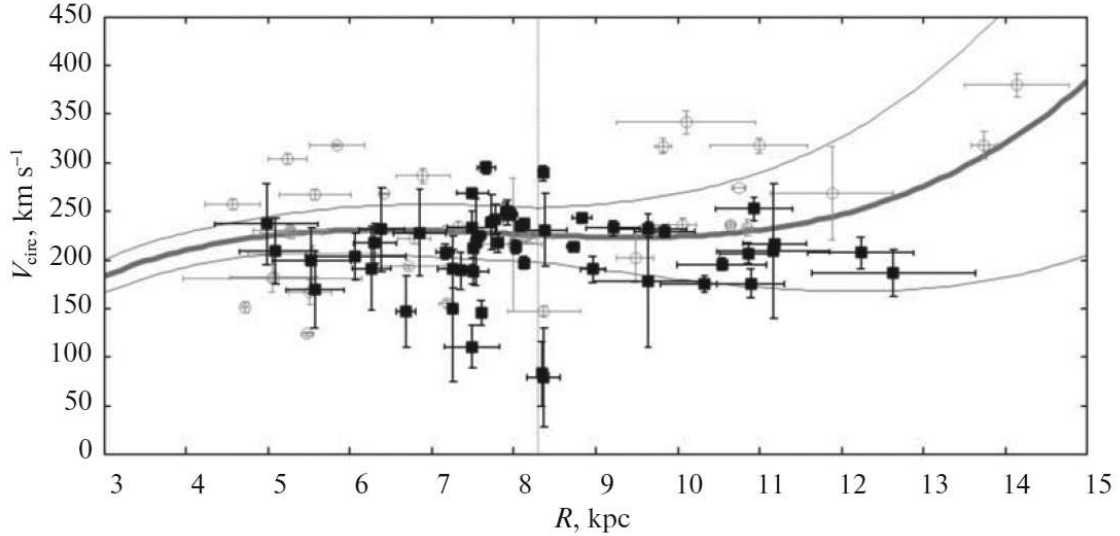


Рис. 4: Circular rotation velocities V_{circ} of PPNe constructed from their total space velocities (filled squares); those constructed only from the PPN line-of-sight velocities (open circles); the Galactic rotation curve found in the solution (24) is indicated by the thick line; the boundaries of the 1σ confidence intervals are marked by the thin lines; the vertical dotted line marks the Sun's position.

$(U \times V \times W) \sim (100 \times 100 \times 100) \text{ km s}^{-1}$, while the second population is concentrated in a ring with a mean radius of $\sim 200 \text{ km s}^{-1}$.

Based on Figs 2 and 3, we can conclude that: (i) when seeking the Galactic rotation parameters based on PPNe, it is better not to use any bulge objects ($R < 4 \text{ kpc}$), which barely rotate and have large velocity errors; (ii) the main group of rotating objects has residual velocities in a compact region with a radius $\sqrt{U^2 + V^2 + W^2}$ less than 200 km s^{-1} ; (iii) the rotating group has velocity deviations ΔV_{circ} no more than 150 km s^{-1} with respect to the flat curve. All of this can be expressed as the following constraints:

$$\begin{aligned} R &> 4 \text{ kpc}, \\ \sqrt{U^2 + V^2 + W^2} &< 200 \text{ km s}^{-1}, \\ \Delta V_{\text{circ}} &< 150 \text{ km s}^{-1}. \end{aligned} \quad (22)$$

Based on the PPNe with the proper motions and line-of-sight velocities, we found the following kinematic parameters from the solution of the conditional equations (15)–(17) using the constraints (22):

$$\begin{aligned} (U_{\odot}, V_{\odot}, W_{\odot}) &= (-9, 29, 11) \pm (6, 8, 6) \text{ km s}^{-1}, \\ \Omega_0 &= 28.3 \pm 3.1 \text{ km s}^{-1} \text{ kpc}^{-1}, \\ \Omega'_0 &= -3.40 \pm 0.63 \text{ km s}^{-1} \text{ kpc}^{-2}, \\ \Omega''_0 &= 0.266 \pm 0.410 \text{ km s}^{-1} \text{ kpc}^{-3}. \end{aligned} \quad (23)$$

In this solution the error per unit weight is $\sigma_0 = 40.5 \text{ km s}^{-1}$, the Oort constants are $A = -14.1 \pm 2.6 \text{ km s}^{-1} \text{ kpc}^{-1}$ and $B = 14.2 \pm 4.1 \text{ km s}^{-1} \text{ kpc}^{-1}$. The solution was found after two iterations with the elimination of large residuals according to the 3σ criterion. We used a total of 145 equations.

Another approach is that the nebulae with the proper motions and line-of-sight velocities give all three equations (15)–(17), the nebulae only with the line-of-sight velocities give one equation (15), and the nebulae only with the measured proper motions give two equations (16) and (17). Using the constraints (22), we found

$$\begin{aligned}
(U_{\odot}, V_{\odot}, W_{\odot}) &= (-1, 30, 10) \pm (5, 6, 5) \text{ km s}^{-1}, \\
\Omega_0 &= 27.8 \pm 2.1 \text{ km s}^{-1} \text{ kpc}^{-1}, \\
\Omega'_0 &= -3.67 \pm 0.46 \text{ km s}^{-1} \text{ kpc}^{-2}, \\
\Omega''_0 &= 0.934 \pm 0.266 \text{ km s}^{-1} \text{ kpc}^{-3}.
\end{aligned}
\tag{24}$$

In this solution the error per unit weight is $\sigma_0 = 44.16 \text{ km s}^{-1}$, the Oort constants are $A = -15.2 \pm 1.9 \text{ km s}^{-1} \text{ kpc}^{-1}$ and $B = 12.5 \pm 2.9 \text{ km s}^{-1} \text{ kpc}^{-1}$, and the circular Galactic rotation velocity at the solar distance is $V_0 = 231 \pm 23 \text{ km s}^{-1}$. We used a total of 208 equations. The solution was found after the elimination of large residuals according to the 3σ criterion. As can be seen, in comparison with the solution (23), the errors in the unknowns decreased here.

There are a total of 57 stars with the proper motions from the Gaia DR1 catalogue (Prusti et al. 2016) in our sample. This catalogue was produced by combining the data in the first year of Gaia observations with the Tycho-2 stellar positions and proper motions (Hog et al. 2000). It is designated as TGAS (Tycho. Gaia Astrometric Solution, Michalik et al. 2015; Brown et al. 2016; Lindegren et al. 2016) and contains the parallaxes and proper motions of ~ 2 million bright stars. The random errors in the parameters included in the Gaia DR1 catalogue are either comparable to or smaller than those in the Hipparcos and Tycho-2 catalogues. The mean parallax errors are ~ 0.3 mas. For most of the TGAS stars the mean proper motion error is 1 mas yr^{-1} , but for quite a few stars common to the Hipparcos catalogue this error is smaller by an order of magnitude, $\sim 0.06 \text{ mas yr}^{-1}$.

Here, we estimate the influence of allowance for the stellar proper motions from the Gaia DR1 catalogue on the kinematic parameters estimated from the entire sample of stars. For this purpose, we use all of the available proper motions and line-of-sight velocities and, where possible, the proper motions from the Gaia DR1 catalogue.

By applying the approach described when seeking the solution (24) using the constraints (22), we found the following parameters:

$$\begin{aligned}
(U_{\odot}, V_{\odot}, W_{\odot}) &= (0, 24, 10) \pm (5, 6, 5) \text{ km s}^{-1}, \\
\Omega_0 &= 27.3 \pm 2.1 \text{ km s}^{-1} \text{ kpc}^{-1}, \\
\Omega'_0 &= -3.69 \pm 0.46 \text{ km s}^{-1} \text{ kpc}^{-2}, \\
\Omega''_0 &= 0.611 \pm 0.264 \text{ km s}^{-1} \text{ kpc}^{-3}.
\end{aligned}
\tag{25}$$

In this solution the error per unit weight is $\sigma_0 = 43.77 \text{ km s}^{-1}$, the Oort constants are $A = -15.3 \pm 1.9 \text{ km s}^{-1} \text{ kpc}^{-1}$ and $B = 12.0 \pm 2.8 \text{ km s}^{-1} \text{ kpc}^{-1}$, and the circular Galactic rotation velocity at the solar distance is $V_0 = 227 \pm 23 \text{ km s}^{-1}$. The solution was found after the elimination of large residuals according to the 3σ criterion. As can be seen, in comparison with the solution (24), the error per unit weight σ_0 decreased here, while the errors in the parameters being determined are the same as those in the solution (24).

To produce the residual velocities, we will apply a flat curve with $V_0 = 227 \text{ km s}^{-1}$. Figure 4 shows the sample of PPNe used in seeking the solution (25) and the Galactic rotation curve found from them. This curve is seen to be close to the flat one in the range of distances R 5–12 kpc.

Note that Bobylev and Bajkova (2017) determined the following Galactic rotation parameters from 226 planetary nebulae at $R_0 = 8.3$ kpc: $(U, V, W)_\odot = (12, 27, 7) \pm (3, 4, 6)$ km s⁻¹, $\Omega_0 = 27.4 \pm 2.6$ km s⁻¹ kpc⁻¹, $\Omega'_0 = -3.47 \pm 0.30$ km s⁻¹ kpc⁻² and $\Omega''_0 = 1.20 \pm 0.26$ km s⁻¹ kpc⁻³, where the linear Galactic rotation velocity at the solar distance is $V_0 = 227 \pm 30$ km s⁻¹. In our view, in comparison with the solutions (24) and (25), the components of the group velocity U_\odot are determined better in this solution.

The situation here is as follows. One reliable determination of the peculiar solar motion relative to the local standard of rest was made by Schönrich et al. (2010), $(U_\odot, V_\odot, W_\odot) = (11.1, 12.2, 7.3) \pm (0.7, 0.5, 0.4)$ km s⁻¹. The lag behind the local standard of rest increases for all older Galactic objects due to an asymmetric drift, i.e., the velocity V_\odot increases. The two other velocities U_\odot and W_\odot remain almost constant in a wide range of stellar ages (Dehnen and Binney 1998). As a result, when producing the residual velocities of PPNe, we suggest using the following values:

$$(U_\odot, V_\odot, W_\odot) = (11.1, 29.7, 7.3) \text{ km s}^{-1}. \quad (26)$$

The Residual Velocities and Their Dispersions

Based on the sample of relatively younger PPNe (with luminosities higher than $5000L_\odot$), we found the following residual velocity dispersions calculated via the roots of the secular equation (11):

$$\begin{aligned} \sigma_1 &= 47 \pm 14 \text{ km s}^{-1}, \\ \sigma_2 &= 41 \pm 8 \text{ km s}^{-1}, \\ \sigma_3 &= 29 \pm 3 \text{ km s}^{-1}, \end{aligned} \quad (27)$$

while the orientation of this ellipsoid is

$$\begin{aligned} L_1 &= 53^\circ, & B_1 &= 15^\circ, \\ L_2 &= 145^\circ, & B_2 &= 7^\circ, \\ L_3 &= 261^\circ, & B_3 &= 74^\circ. \end{aligned} \quad (28)$$

This solution was obtained using 222 equations in the system of conditional equations (5)–(10).

Based on the sample of PPNe with luminosities of $4000 L_\odot$ and $3500 L_\odot$, we found the following residual velocity dispersions:

$$\begin{aligned} \sigma_1 &= 50 \pm 17 \text{ km s}^{-1}, \\ \sigma_2 &= 38 \pm 22 \text{ km s}^{-1}, \\ \sigma_3 &= 28 \pm 33 \text{ km s}^{-1}, \end{aligned} \quad (29)$$

while the orientation of this ellipsoid is

$$\begin{aligned} L_1 &= 72^\circ, & B_1 &= 11^\circ, \\ L_2 &= 161^\circ, & B_2 &= -16^\circ, \\ L_3 &= 345^\circ, & B_3 &= 71^\circ. \end{aligned} \quad (30)$$

This solution was obtained using 127 equations in the system of conditional equations (5)–(10).

Finally, we analyzed the sample of PPNe with luminosities of $1700 L_\odot$. According to the classification by Vickers et al. (2015), some of them belong to the thick disk (with

metallicities [Fe/H] in the range from -1.6 to -0.3 dex), but they are mostly Galactic halo objects. Based on this sample, we found the following residual velocity dispersions:

$$\begin{aligned}\sigma_1 &= 91 \pm 21 \text{ km s}^{-1}, \\ \sigma_2 &= 49 \pm 25 \text{ km s}^{-1}, \\ \sigma_3 &= 36 \pm 9 \text{ km s}^{-1},\end{aligned}\tag{31}$$

while the orientation of this ellipsoid is

$$\begin{aligned}L_1 &= 27^\circ, & B_1 &= -2^\circ, \\ L_2 &= 117^\circ, & B_2 &= -6^\circ, \\ L_3 &= 96^\circ, & B_3 &= 84^\circ.\end{aligned}\tag{32}$$

This solution was obtained using 92 equations in the system of conditional equations (5)–(10).

The solutions (27)–(31) were obtained under identical constraints. More specifically, the heliocentric distances of the nebulae did not exceed 8 kpc, the bulge objects ($R > 4$ kpc) were eliminated, the magnitude of each of the velocities U , V , or W did not exceed 300 km s $^{-1}$ (see Fig. 3), and, finally, the proper motions were used only up to heliocentric distances of 4 kpc (because the proper motion errors increase with distance).

It is interesting to compare our estimates with the results of the analysis of white dwarfs from Pauli et al. (2006), where the following velocity dispersions were determined: $(\sigma_U, \sigma_V, \sigma_W) = (34, 24, 18)$ km s $^{-1}$ for a sample of 361 thin-disk white dwarfs, $(\sigma_U, \sigma_V, \sigma_W) = (79, 36, 46)$ km s $^{-1}$ for a sample of 27 thick-disk white dwarfs, and $(\sigma_U, \sigma_V, \sigma_W) = (138, 95, 47)$ km s $^{-1}$ for a sample of 7 halo white dwarfs. A direct comparison with the results that we obtained above is difficult to make, because $(\sigma_U, \sigma_V, \sigma_W)$ are the residual velocity dispersions directed along the (x, y, z) coordinate axes, while the ellipsoids (28)–(32) occasionally have significant deviations from the directions of the x and y coordinate axes.

On the whole, we can conclude that there is a good correlation between the spatial and kinematic properties of PPNe and their separation in luminosity proposed by Vickers et al. (2015).

CONCLUSIONS

We supplemented the catalogue of PPNe by Vickers et al. (2015) with a homogeneous distance scale by the line-of-sight velocities and proper motions of their central stars from the literature.

An exponential density distribution was used to analyze the vertical distribution of PPNe. We considered two samples of objects from a solar neighborhood with a radius of 6 kpc separated in age using the luminosity indices from the catalogue by Vickers et al. (2015). Based on a sample of 107 objects with an age less than 3 Gyr belonging to the Galactic thin disk, we estimated the vertical scale height to be $h = 146 \pm 15$ pc. Based on a sample of 88 older objects, we found $h = 568 \pm 42$ pc, a value typical for Galactic thick-disk objects.

We compiled a list of 147 PPNe in which there are only the line-of-sight velocities for 55 nebulae, only the proper motions for 25 nebulae, and both line-of-sight velocities and proper motions for 67 nebulae. For a number of stars the proper motions were taken from the Gaia DR1 catalogue. Based on this kinematic sample, we obtained the following Galactic rotation parameters: $(U_\odot, V_\odot, W_\odot) = (0, 24, 10) \pm (5, 6, 5)$ km s $^{-1}$, $\Omega_0 = 27.3 \pm 2.1$ km s $^{-1}$ kpc $^{-1}$,

$\Omega'_0 = -3.69 \pm 0.46 \text{ km s}^{-1} \text{ kpc}^{-2}$, and $\Omega''_0 = 0.611 \pm 0.264 \text{ km s}^{-1} \text{ kpc}^{-3}$ for the adopted $R_0 = 8.3 \text{ kpc}$. The Oort constants are $A = -15.3 \pm 1.9 \text{ km s}^{-1} \text{ kpc}^{-1}$ and $B = 12.0 \pm 2.8 \text{ km s}^{-1} \text{ kpc}^{-1}$, while the circular rotation velocity at the solar distance is $V_0 = 227 \pm 23 \text{ km s}^{-1}$.

We showed that there is a good correlation between the kinematic properties of nebulae and their separation in luminosity proposed by Vickers et al. (2015). For example, the following principal semiaxes of the residual velocity dispersion ellipsoid have been found: $(\sigma_1, \sigma_2, \sigma_3) = (47, 41, 29) \text{ km s}^{-1}$ from a sample of relatively young PPNe (with luminosities higher than $5000 L_\odot$), $(\sigma_1, \sigma_2, \sigma_3) = (50, 38, 28) \text{ km s}^{-1}$ from a sample of older PPNe (with luminosities of $4000 L_\odot$ or $3500 L_\odot$), and, finally, $(\sigma_1, \sigma_2, \sigma_3) = (91, 49, 36) \text{ km s}^{-1}$ from the oldest halo nebulae (with luminosities of $1700 L_\odot$).

ACKNOWLEDGMENTS

We are grateful to the referee for the helpful remarks that contributed to an improvement of this paper. This work was supported by the Basic Research Program P-7 of the Presidium of the Russian Academy of Sciences, the ‘‘Transitional and Explosive Processes in Astrophysics’’ Subprogram.

REFERENCES

1. C. Allen and A. Santillán, *Rev. Mex. Astron. Astrofis.* 22, 255 (1991).
2. V. P. Arkhipova, N. P. Ikonnikova, R. I. Noskova, G. V. Komissarova, V. G. Klochkova, and V. F. Esipov, *Astron. Lett.* 27, 719 (2001).
3. A. T. Bajkova and V. V. Bobylev, *Baltic Astron.* 24, 43 (2015).
4. V. V. Bobylev and A. T. Bajkova, *Astron. Lett.* 39, 809 (2013).
5. V. V. Bobylev and A. T. Bajkova, *Astron. Lett.* 40, 389 (2014).
6. V. V. Bobylev and A. T. Bajkova, *Astron. Lett.* 42, 1 (2016).
7. V. V. Bobylev and A. T. Bajkova, *Astron. Lett.* 43, (2017, in press).
8. C. Bonatto, L. O. Kerber, E. Bica, and B. X. Santiago, *Astron. Astrophys.* 446, 121 (2006).
9. J. Bovy, H.-W. Rix, and D. W. Hogg, *Astrophys. J.* 751, 131 (2012).
10. J. Bovy, H.-W. Rix, E. F. Schlafly, D. L. Nidever, J. A. Holtzman, M. Shetrone, and T. C. Beers, *Astrophys. J.* 823, 30 (2016).
11. A. G. A. Brown, A. Vallenari, T. Prusti, J. de Bruijne, F. Mignard, R. Drimmel, et al. (GAIA Collab.), *Astron. Astrophys.* 595, A2 (2016).
12. A. S. M. Buckner and D. Froebrich, *Mon. Not. R. Astron. Soc.* 444, 290 (2014).
13. L. Chen, M. Geffert, J. J. Wang, K. Reif, and J. M. Braun, *Astron. Astrophys. Suppl. Ser.* 145, 223 (2000).
14. B. Chen, C. Stoughton, J. A. Smith, A. Uomoto, J. R. Pier, B. Yanny, Ž.E. Ivezić, D. G. York, et al., *Astrophys. J.* 553, 184 (2001).
15. R. M. Deacon, J. M. Chapman, and A. J. Green, *Astrophys. J. Suppl. Ser.* 155, 595 (2004).
16. V. P. Debattista, O. Gerhard, and M. N. Sevenster, *Mon. Not. R. Astron. Soc.* 334, 355 (2002).
17. W. Dehnen and J. J. Binney, *Mon. Not. R. Astron. Soc.* 298, 387 (1998).
18. D. Engels and F. Bunzel, *Astron. Astrophys.* 582, A68 (2015).
19. D. S. Evans, in *Proceedings of the IAU Symposium No. 30*, Toronto, Canada (1979), p. 57.
20. D. J. Frew, PhD Thesis (Dep. Physics, Macquarie Univ., NSW 2109, Australia, 2008).
21. P. Garcia-Lario, A. Manchado, W. Pych, and S. R. Pottasch, *Astron. Astrophys. Suppl. Ser.* 126, 479 (1997).
22. P. Garcia-Lario, in *Planetary Nebulae in our Galaxy and Beyond*, *Proceedings of the IAU Symposium No. 234*, Ed. by M. J. Barlow and R. H. Méndez (2006).

23. K. Gesicki, A. A. Zijlstra, M. Hajduk, and C. Szyszka, *Astron. Astrophys.* 566, A48 (2014).
24. S. Gillessen, F. Eisenhauer, T. K. Fritz, H. Bartko, K. Dodds-Eden, O. Pfuhl, T. Ott, and R. Genzel, *Astroph. J.* 707, L114 (2009).
25. J. F. Gómez, J. R. Rizzo, O. Suárez, A. Palau, L. F. Miranda, M. A. Guerrero, G. Ramos-Larios, and J. M. Torrelles, *Astron. Astrophys.* 578, 119 (2015).
26. H. J. Habing and H. Olofsson, *Asymptotic Giant Branch Stars* (Springer, New York, Berlin, 2003).
27. The HIPPARCOS and Tycho Catalogues, ESA SP-1200 (1997).
28. E. Hog, A. Kuzmin, U. Bastian, C. Fabricius, K. Kuimov, L. Lindegren, V. V. Makarov, and S. Roeser, *Astron. Astrophys.* 335, L65 (1998).
29. E. Hog, C. Fabricius, V. V. Makarov, U. Bastian, P. Schwekendiek, A. Wicenec, S. Urban, T. Corbin, and G. Wycoff, *Astron. Astrophys.* 355, L27 (2000).
30. H. Imai, R. Sahai, and M. Morris, *Astrophys. J.* 669, 424 (2007).
31. H. Imai, T. Kurayama, M. Honma, and T. Miyaji, *Astrophys. J.* 771, 47 (2013).
32. N. V. Kharchenko, R.-D. Scholz, A. E. Piskunov, S. Röser, and E. Schilbach, *Astron. Nachr.* 328, 889 (2007).
33. N. V. Kharchenko, A. E. Piskunov, E. Schilbach, S. Röser, and R.-D. Scholz, *Astron. Astrophys.* 558, A53 (2013).
34. V. G. Klochkova, R. Szczerba, V. E. Panchuk, and K. Volk, *Astron. Astrophys.* 345, 905 (1999).
35. V. G. Klochkova, E. L. Chentsov, N. S. Tavelzhanskaya, and V. E. Panchuk, *Astron. Rep.* 51, 642 (2007).
36. V. G. Klochkova, *Astron. Lett.* 39, 765 (2013).
37. V. G. Klochkova, E. L. Chentsov, V. E. Panchuk, E. G. Sendzikas, and M. V. Yushkin, *Astrophys. Bull.* 69, 439 (2014).
38. V. G. Klochkova, V. E. Panchuk, and N. S. Tavelzhanskaya, *Astron. Lett.* 41, 14 (2015).
39. F. van Leeuwen, *Astron. Astrophys.* 474, 653 (2007).
40. L. Lindegren, U. Lammers, U. Bastian, J. Hernandez, S. Klioner, D. Hobbs, A. Bombrun, D. Michalik, et al., *Astron. Astrophys.* 595, A4 (2016).
41. S. R. Majewski, *Astron. Nachr.* 337, 863 (2016).
42. D. R. C. Mello, S. Daflon, C. B. Pereira, and I. Hubeny, *Astron. Astrophys.* 543, 11 (2012).
43. D. Michalik, L. Lindegren, and D. Hobbs, *Astron. Astrophys.* 574, A115 (2015).
44. C. J. Mooney, W. R. J. Rolleston, F. P. Keenan, P. L. Dufton, J. V. Smoker, R. S. I. Ryans, and L. H. Aller, *Mon. Not. R. Astron. Soc.* 337, 851 (2002).
45. G. Neugebauer, B. T. Soifer, G. Miley, H. J. Habing, E. Young, F. J. Low, C. A. Beichman, P. E. Clegg, et al., *Astrophys. J.* 278L, 83 (1984).
46. K. F. Ogorodnikov, *Dynamics of Stellar Systems* (Fizmatgiz, Moscow, 1965) [in Russian].
47. E.-M. Pauli, R. Napiwotzki, U. Heber, M. Altmann, and M. Odenkirchen, *Astron. Astrophys.* 447, 173 (2006).
48. A. F. Pérez-Sánchez, W. H. T. Vlemmings, D. Tafuya, and J. M. Chapman, *Mon. Not. R. Astron. Soc.* 436, L79 (2013).
49. T. Prusti, J. H. J. de Bruijne, A. G. A. Brown, A. Vallenari, C. Babusiaux, C. A. L. Bailer-Jones, U. Bastian, M. Biermann, et al. (GAIA Collab.), *Astron. Astrophys.* 595, A1 (2016).
50. S. S. Rao, S. Giridhar, and D. L. Lambert, *Mon. Not. R. Astron. Soc.* 419, 1254 (2012).
51. A. S. Rastorguev, M. V. Zabolotskikh, A. K. Dambis, N. D. Utkin, A. T. Bajkova, and V. V. Bobylev, *Astrophys. Bull.* 72, 122 (2017).
52. M. J. Reid, K. M. Menten, A. Brunthaler, X. W. Zheng, T. M. Dame, Y. Xu, Y. Wu, B. Zhang, et al., *Astrophys. J.* 783, 130 (2014).
53. M. Reyniers and H. van Winckel, *Astron. Astrophys.* 365, 465 (2001).
54. H.-W. Rix and J. Bovy, *Astron. Astrophys. Rev.* 21, 61 (2013).

55. R. S. I. Ryans, P. L. Dufton, F. P. Keenan, S. J. Smartt, K. R. Sembach, D. J. Lennon, and K. A. Venn, *Astrophys. J.* 490, 267 (1997).
56. C. Sánchez Contreras and R. Sahai, *Astrophys. J. Suppl. Ser.* 203, 16 (2012).
57. R. Schönrich, J. Binney, and W. Dehnen, *Mon. Not. R. Astron. Soc.* 403, 1829 (2010).
58. L. Stanghellini and M. Haywood, *Astrophys. J.* 714, 1096 (2010).
59. O. Suárez, P. Garcia-Lario, A. Manchado, M. Manteiga, A. Ulla, and S. R. Pottasch, *Astron. Astrophys.* 458, 173 (2006).
60. R. Szczerba, N. Siodmiak, G. Stasińska, and J. Borkowski, *Astron. Astrophys.* 469, 799 (2007).
61. R. Szczerba, N. Siodmiak, G. Stasińska, J. Borkowski, P. Garcia-Lario, O. Suárez, M. Hajduk, and D. A. Garcia-Hernández, in *Planetary Nebulae: An Eye to the Future*, Proceedings of the IAU Symposium No 283, Ed. by A. Manchado, L. Stanghellini and D. Schönberner (2012), p. 506.
62. R. J. Trumpler and H. F. Weaver, *Statistical Astronomy* (Univ. of California Press, Berkely, 1953).
63. S. Vennes, R. J. Smith, B. J. Boyle, S. M. Croom, A. Kawka, T. Shanks, L. Miller, and N. Loaring, *Mon. Not. R. Astron. Soc.* 335, 673 (2002).
64. S. B. Vickers, D. J. Frew, Q. A. Parker, and I. S. Bojičić, *Mon. Not. R. Astron. Soc.* 447, 1673 (2015).
65. D.-H. Yoon, S.-H. Cho, J. Kim, Y. J. Yun, and Y.-S. Park, *Astrophys. J. Suppl. Ser.* 211, 15 (2014).
66. N. Zacharias, S. E. Urban, M. I. Zacharias, G. L. Wycoff, D. M. Hall, M. E. Germain, E. R. Holdenried, and L. Winter, *Astron. J.* 127, 3043 (2004).
67. N. Zacharias, C. T. Finch, T. M. Girard, N. Hambly, G. Wycoff, M. I. Zacharias, D. Castillo, T. T. Corbin, et al., *Astron. J.* 139, 2184 (2010).
68. N. Zacharias, C. T. Finch, T. M. Girard, A. Henden, J. L. Bartlett, D. G. Monet, and M. I. Zacharias, *Astron. J.* 145, 44 (2013).